Plethodontid modulating factor, a hypervariable salamander courtship pheromone in the three-finger protein superfamily

Catherine A. Palmer[1], David M. Hollis[1], Richard A. Watts[1], Lynne D. Houck[1], Maureen A. McCall[2], Ronald G. Gregg[3], Pamela W. Feldhoff[3], Richard C. Feldhoff[3] and Stevan J. Arnold[1]

1 Department of Zoology, Oregon State University, Corvallis, OR, USA
2 Department Psychological and Brain Sciences, University of Louisville, KY, USA
3 Department Biochemistry and Molecular Biology, School of Medicine, University of Louisville, KY, USA

The soluble members of the three-finger protein superfamily all share a relatively simple 'three-finger' structure, yet perform radically different functions. Plethodontid modulating factor (PMF), a pheromone protein produced by the lungless salamander, *Plethodon shermani*, is a new and unusual member of this group. It affects female receptivity when delivered to the female's nares during courtship. As with other plethodontid pheromone genes, PMF is hyperexpressed in a specialized male mental (chin) gland. Unlike other plethodontid pheromone genes, however, PMF is also expressed at low levels in the skin, liver, intestine and kidneys of both sexes. The PMF sequences obtained from all tissue types were highly variable, with 103 unique haplotypes identified which averaged 35% sequence dissimilarity (range 1–60%) at the protein level. Despite this variation, however, all PMF sequences contained a conserved ≈ 20-amino-acid secretion signal sequence and a pattern of eight cysteines that is also found in cytotoxins and short neurotoxins from snake venoms, as well as xenoxins from *Xenopus*. Although they share a common cysteine pattern, PMF isoforms differ from other three-finger proteins in: (a) amino-acid composition outside of the conserved motif; (b) length of the three distinguishing 'fingers'; (c) net charge at neutral pH. Whereas most three-finger proteins have a net positive charge at pH 7.0, PMF has a high net negative charge at neutral pH (pI range of most PMFs 3.5–4.0). Sequence comparisons suggest that PMF belongs to a distinct multigene subfamily within the three-finger protein superfamily.

The proteins in the three-finger protein superfamily are highly variable but all share a relatively simple structure termed a 'three-finger' fold. This three-dimensional structure consists of three adjacent 'finger-like' loops extending from a small, hydrophobic core that is cross-linked by a common disulfide bond bridging pattern (see review [1]). The three-finger proteins (TFPs) are widespread, and both soluble and membrane-bound members have been described in detail (refer to [1–3] for original references).

TFPs have very diverse functions and exhibit an extraordinary degree of tissue and taxon specificity [4]. This functional diversity is well illustrated within families of TFPs, such as the family of three-finger toxins

found in elapid and colubrine snakes [5–7]. Representative three-finger toxins from these snake venoms include long-chain and short-chain neurotoxins, fasciculins, cardiotoxins and muscarinic toxins [5]. Whereas α-neurotoxins bind selectively to the nicotinic acetylcholine receptor (nAChR) to block neuromuscular transmission [8], fasciculins work to inhibit acetylcholinesterases [9], and muscarinic toxins interact with muscarinic acetylcholine receptors [10]. Cardiotoxins act in a very different manner in that they cause lysis of erythrocytes and lymphocytes, trigger contraction of cardiac muscle, and inhibit certain enzymes [11].

Consideration of the nontoxin proteins in the TFP superfamily further highlights the great functional plasticity of the three-finger fold [3]. Some soluble TFPs in this group, for example, are potent neuromodulators for epidermal homeostasis (e.g. SLURP-1 [12]). Other TFPs activate Ca^{2+} channels in epithelial cells (e.g. xenoxin [13]), or enhance sperm motility by inhibiting Ca^{2+} transport into spermatozoa (e.g. SVS-VII/caltrin [14]). The membrane-bound members of the TFP superfamily protect cells from the membrane attack complex (e.g. CD59 [15]), play a vital role in T-lymphocyte activation (e.g. Ly-6 [16]) and early development (e.g. TSA-1 [17]), underlie a variety of pathological processes such as metastasis, inflammation and tumor invasion (e.g. uPAR; a receptor consisting of three distinct TFP-like domains [18]), or act as modulators for nAChRs in the brain (e.g. Lynx1 [19]). From protection against destruction of cells, to roles in reproduction, development, disease, and immune response, the TFP superfamily illustrates remarkable conservation of an ancient protein scaffold that has evolved to use different combinations of amino acids to generate a wide variety of functions.

Our observation that the pheromone protein plethodontid modulating factor (PMF) is a TFP extends the known functional diversity of the TFP superfamily. The PMF protein is a major constituent of the courtship pheromone that is secreted from the chin (mental) glands of sexually active male salamanders of the family Plethodontidae. The pheromone blend also includes plethodontid receptivity factor (PRF), a protein that is structurally related to interleukin-6-type cytokines [20] and sodefrin precursor-like factor, a phospholipase A2 inhibitor-like protein [21]. During the courtship of certain species of salamander, such as the red-legged salamander, *Plethodon shermani*, the male dabs his mental gland across the female's nares in a 'slapping' motion [22]. This slapping behavior results in pheromone delivery to the female's vomeronasal organ (VNO) and subsequent activation of VNO receptor neurons [23–25]. VNO neurons then project to a region of the

accessory olfactory bulb known to initiate reproductive responses in vertebrates [26,27]. Behavioral bioassays reveal that PMF modulates the female's response to male courtship behavior [28].

Previous biochemical analyses reported PMF (previously named Pj-7 and Pj-10) to be a 7-kDa protein present in extracts of the male mental gland in a 2 : 1 ratio with PRF [29,30]. This 2 : 1 (PMF/PRF) ratio was consistent for gland extracts prepared in different years [29]. HPLC suggested the existence of multiple PMF isoforms, four of which were partially characterized (unpublished data) through amino-acid sequencing of 20–30 N-terminal residues and preliminary cloning experiments [30]. In this article, we focus on a single population of the red-legged salamander, *P. shermani*, with the aims of: (a) further analyzing the biochemical characteristics of PMF; (b) determining the sites of expression of PMF; (c) characterizing the range of PMF variation that is expressed in a single population; (d) evaluating sequence similarities and differences between PMF and other related, well-known TFPs. In a later report, we plan to examine PMF sequence differences in salamander species that are closely and distantly related to *P. shermani*. That report will also include a detailed discussion of PMF's evolution.

Results

PMF is a hypervariable multigene family expressed in several salamander tissues

Comparisons of randomly sequenced *P. shermani* mental gland cDNA clones with N-terminal sequences from purified PMF isoforms identified multiple unique PMF clones (supplementary Fig. S1). Tissues from sexually active male and female *P. shermani*, as well as from the homogenized whole bodies of juvenile salamanders, were then surveyed for the presence of PMF transcripts (Table 1). PMF sequences were isolated from male mental glands and from the skin, liver, intestine and kidneys of adult salamanders of both sexes. PMF sequences were not detected in the heart, tail tip or female chin skin of adults, nor were they isolated from the bodies of juvenile salamanders.

Sequencing of 248 PMF clones yielded 103 unique haplotypes (Table 1). PMF nucleotide sequence length varied from 231 to 258 bp (77–86 amino acids, which includes a 19-amino-acid secretion signal) with 161 polymorphic sites. Standard translation of these nucleotide sequences resulted in 81 unique amino-acid sequences that all shared a highly conserved signal sequence (residues −1 to −19) and a set of mature PMF sequences that was extremely diverse in terms of

Table 1. RT-PCR results for PMF nucleotide sequence and amino-acid sequence dissimilarity in various *P. shermani* male and female tissues. VT, Skin surrounding the vent; DT, skin from the dorsal tail-base region. Note: The totals for unique haplotypes and unique translations cannot be determined by addition because, in some instances, identical PMF sequences were isolated from both sexes.

Tissue sample	No. of animals	Clones sequenced	Unique haplotypes	Nucleotide sequence dissimilarity (%)	Unique translations	Amino acid sequence dissimilarity (%)
Male						
All	3	162	65	18.7 ± 1.7	54	38.3 ± 5.1
VT	3	29	16	19.6 ± 1.8	15	41.4 ± 4.9
DT	3	28	14	21.1 ± 2.1	13	40.6 ± 5.8
Mental gland	3	79	35	17.3 ± 1.7	27	36.7 ± 5.1
Intestine	1	8	5	23.7 ± 2.8	5	45.6 ± 6.3
Kidney	1	8	2	0.4 ± 0.4	1	n/a
Liver	1	10	2	0.4 ± 0.4	2	1.2 ± 1.2
Female						
All	5	86	44	15.9 ± 1.7	37	30.3 ± 4.4
VT	4	30	11	15.5 ± 1.6	8	32.1 ± 5.1
DT	4	30	23	11.7 ± 1.5	19	23.2 ± 3.5
Intestine	1	8	1	n/a	1	n/a
Kidney	1	10	10	21.6 ± 2.1	8	36.5 ± 5.1
Liver	1	8	3	19.6 ± 2.4	3	37.0 ± 6.0
Total	8	248	103	17.8 ± 1.8	81	34.6 ± 5.1

residue composition and deletion/insertion patterns (Fig. 1; supplementary Fig. S1). Deletions of various length were present in 36% of the sequences at positions 14, 16–18, 28, 43–48, and/or 53–54 (see Fig. 1 using PMF male intestine as the reference). A three-amino-acid insertion was present at the N-terminus of one sequence and a single residue insertion was found

immediately following the asparagine at the C-terminus in 3% of the sequences (supplementary Fig. S1). The latter is also a common characteristic of TFPs.

Sequence dissimilarity across all PMF sequences was ≈18% and 35% at the nucleotide and protein levels, respectively (Table 1). Substitutions were concentrated on first and second bases of the codons, resulting in a
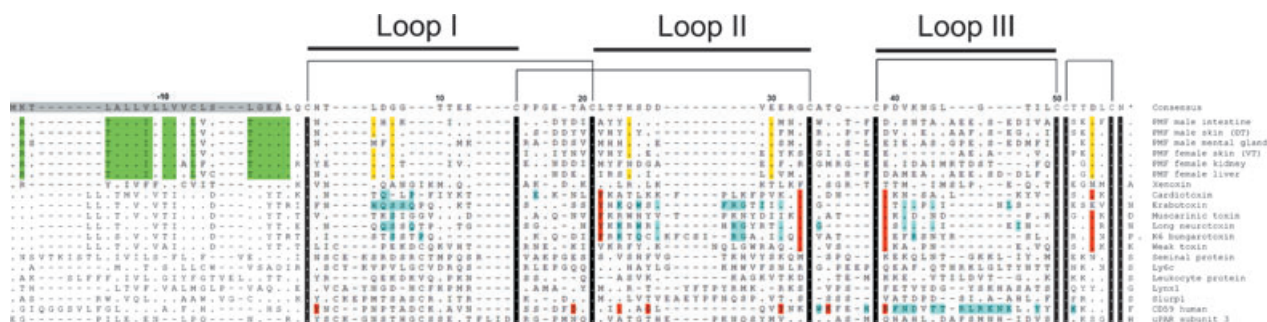
Fig. 1. Representative amino-acid sequences of PMF and related TFPs. The dots represent amino-acid residues that are identical with the consensus sequence, whereas dashes represent gaps in the sequences. Residues strictly conserved within the TFP family are given against a black background. Highly conserved residues within PMF (> 95%) are given against a green background, and residues conserved across 90% of the PMF sequences are in yellow. Functionally important amino-acid residues are highlighted in blue, and those highlighted in red represent amino acids that are structurally important (Cys residues excluded) [2,31–37]. VT, Skin from around the vent; DT, skin from the dorsal tail-base region. The secretion signal is shown against a grey background on the consensus sequence. The CD59 and snake long-chain neurotoxins have been truncated at the site equivalent to the soluble TFP/PMF stop codon. GenBank accession numbers for these sequences are as follows: *P. shermani* PMF male intestine (DQ882329); PMF male skin (DT) (DQ882308); PMF male mental gland (DQ882251); PMF female skin (VT) (DQ882331); PMF female kidney (DQ882367); PMF female liver (DQ882377); xenoxin, *Xenopus laevis* (CAA51225); cardiotoxin, *Naja atra* (CAA90964); erabutoxin, *Laticauda semifasciata* (CAA35770); muscarinic toxin, *Dendroaspis angusticeps* (1801365 A); long neurotoxin (α-cobrotoxin), *Naja kaouthia* (AAY63884); k-6 bungarotoxin, *Bungarus multicinctus* (CAB46659); weak toxin, *Bungarus candidus* (AAL30059); seminal protein caltrin, *Mus musculus* (NP_064660); Ly6c, *Homo sapiens* (NP_079537); leucocyte protein, *Eptatretus stoutii* (AAD47892); Lynx1, *Mus musculus* (Q9WVC2); SLURP-1, *Homo sapiens* (P55000); CD59 antigen, *Homo sapiens* (NP_976074); uPAR subunit three, *Homo sapiens* (Q03405).

large number of amino-acid (nonsynomyous) changes (Table 1). Only 24 of 70 shared amino-acid residues were highly conserved (> 95%) across the 81 unique sequences. Fourteen of these 24 conserved residues were located in the secretion signal peptide (Fig. 1). The other 10 conserved residues included a leucine at the first amino-acid position, an asparagine at the C-terminus, and eight cysteines, which probably provide protein conformational stability via the formation of disulfide bridges. Residues Leu6, Gly8, Lys25, Glu30 and Asp54 (Fig. 1, consensus) were conserved across 90% of the PMF sequences and may play important structural and/or functional roles. The remaining 41 shared amino-acid positions ($\approx$ 60% of the protein) were highly variable. Many of these non-conserved positions had at least six different amino-acid changes, including substitutions with functionally different side chains. Position 41 (Fig. 1; consensus) had 11 different amino-acid substitutions and was the most variable site on the protein.

Multiple tissue types in adult *P. shermani* express a similar set of highly variable PMF transcripts. Sequencing of 40 clones from a single RT-PCR on mental gland tissue extracts from one male resulted in 26 unique PMF nucleotide sequences, suggesting that at least 13 PMF genes are expressed in the gland. Average PMF nucleotide dissimilarity for this individual gland was 20.5% ($\pm$ 2.5%), with $\approx$ 37% ($\pm$ 5%) dissimilarity at the protein level. The mental gland was more extensively sampled than other tissue types, but PMF sequence variation was also high in most other adult tissues (see Table 1). Although relatively few haplotypes were detected in some tissues (e.g. liver), a regression analysis indicates that 94% of the among-tissue variation in the number of unique haplotypes was a function of sampling effort (data not shown). There was no evidence of tissue or gender specificity for PMF haplotypes. In fact, 14 PMF haplotypes isolated from male mental gland tissue were also detected in the skin of both sexes. Furthermore, PMF sequence variation was as great within tissues as it was between tissues in most cases (data not shown).

Mental gland cDNA library results indicate that we have not captured all of the variation in PMF

Approximately 300 clones were randomly sequenced from a cDNA mental gland library constructed from 10 *P. shermani* males from a single population. Of these, 120 clones encoded ORFs in the PMF family. Forty-two different nucleotide sequences were represented in these 120 clones. Average nucleotide dissimi-larity among these library PMF sequences was 37% ($\pm$ 3.2%), with $\approx$ 65% protein sequence dissimilarity among them. Many sequences from this library were also detected using RT-PCR methods, but nearly 8% of the sequences were not. The ongoing detection of novel and highly variable PMF sequences indicates that we have not yet captured all of the variation in this protein family.

PMF is hyperexpressed in the male mental gland

On the basis of *in situ* hybridization (ISH) procedures and the use of a PMF antisense riboprobe, PMF is highly expressed only within the mental gland of male *P. shermani*. Labeling was distributed throughout the gland and was lightest in the center of the tissue, with intensity increasing to its most intense along the outer reaches just inside the dermis (stratum spongiosum; Fig. 2). Labeling also occurred in the cells of the dermis immediately adjacent to highly labeled glands, but with much less intensity (Fig. 2). Tissues probed with the sense strand of the PMF sequences were devoid of any labeling above background in all tissue samples.

Distinct PMF ISH labeling was not observed in sections of adult skin that were isolated from the dorsal tail-base region or from around the vent, possible sites of pheromone production and release. Furthermore, frontal sections traversing the entire length of the body of juveniles showed no observable PMF ISH labeling in any juvenile tissue. These results combined with our RT-PCR findings suggest that PMF is present in the skin of adult salamanders but is expressed at very low levels. In contrast, ISH results suggest that PMF is highly expressed in the male's mental gland.

### PMF shares structural features with the TFP superfamily

Several proteins related to PMF were identified in BLASTX searches on GenBank. These related proteins included the XLURP-1 (AAK52825) and xenoxin (CAA51225) proteins from *Xenopus laevis*, the CD59 antigen (AAP36795) and SLURP-1 (AAT01436) genes of *Homo sapiens*, weak toxins (AAL30060, AAL30059) and a neurotoxin (CAA72941) from elapid snakes (*Bungarus* spp.), and an undescribed protein from *Caenorhabditis elegans* (NP_508284). Overall PMF amino-acid identity with these proteins is low, ranging from 27% to 30%. However, these proteins all belong to the TFP superfamily, which is characterized by the presence of a cysteine-rich domain. This domain contains 8–10 cysteine residues with highly conserved
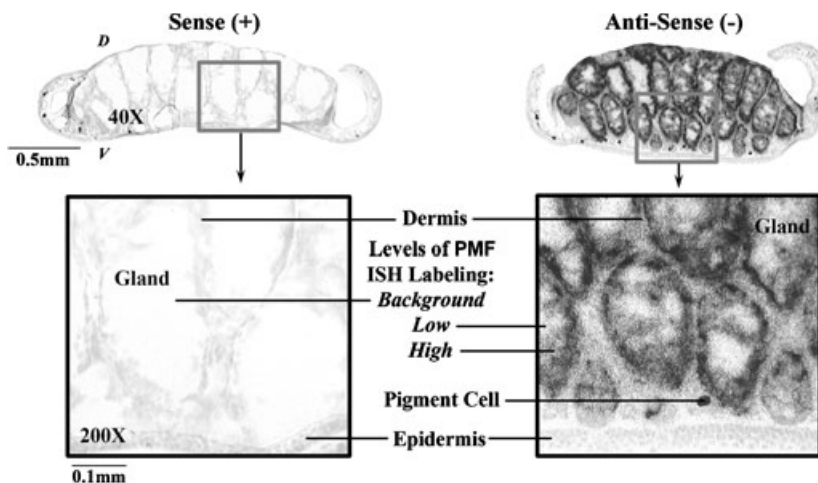
Fig. 2. PMF ISH labeling in the mental gland of an adult male *P. shermani* using a PMF-specific ³⁵S-labeled riboprobe. Top, low-magnification (40×) photomicrographs of the mental gland incubated with either the sense probe (negative control; left) or the antisense probe (right). Bottom, high resolution (200×) of the mental gland indicating regional specificity of PMF ISH labeling.

spacing and a characteristic C-C-X-X-X-X-C-N at the C-terminus. The 8-Cys domain is also present in PMF (Fig. 1). For members of the TFP superfamily for which structures have been determined, the 8-Cys domain forms disulfide bridges at Cys3-Cys21, Cys14-Cys34, Cys38-Cys50 and Cys51-Cys56 (Fig. 1; consensus) and results in a characteristic TFP fold [3]. A protein alignment of PMF with members of this superfamily (Fig. 1) reveals considerable amino-acid diversity tightly bracketed by this conserved scaffold of cysteine residues.

The RAPTOR threading program [38] was used to predict the folding structure of PMF using the primary sequence as input. RAPTOR threading results consistently matched PMF with members of the TFP superfamily. Structural templates for PMF, with their associated E-values and PDB accession numbers, included the snake toxins, γ-bungarotoxin (1.32 E^{-02}; 1MR6) and candotoxin (1.48 E^{-02}; 1JGK) from *Bungarus*, as well as the complement regulatory protein (CD59) from *Homo sapiens* (1.13 E^{-01}; 1CDQ). An important structural difference between these proteins and PMF is that the three template proteins all have a fifth disulfide bridge at the tip of loop I that is not present in PMF. The molecular dynamics algorithms of the Insight II modelling software used cardiotoxin V as a reference to calculate a 'threaded' theoretical structure for PMF. Figure 3 shows the PMF structure superimposed over the crystal structure for cardiotoxin V. In this example, both proteins have four distinct disulfide bridges. Although PMF is predicted to be primarily a β-sheet structure and to have the classic three-finger fold, the substantial sequence and charge
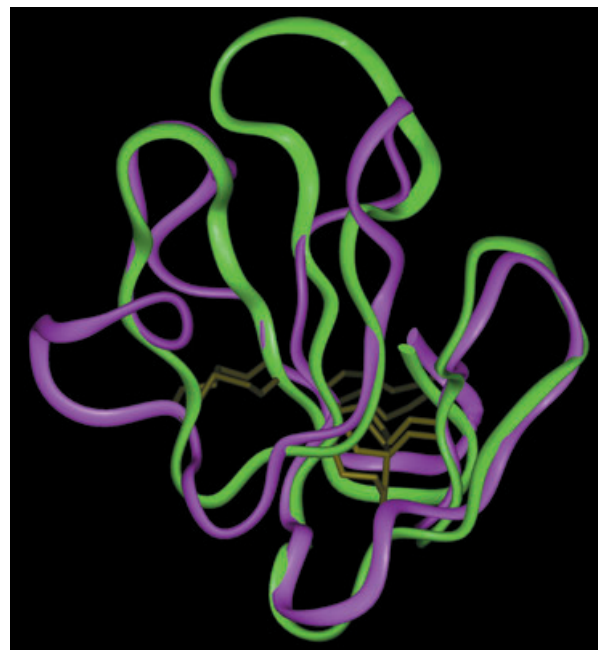
Fig. 3. Theoretical structural model of PMF (GenBank accession No. ABI48573) from the mental gland of the terrestrial salamander (*P. shermani*) superimposed over the crystal structure for cardiotoxin V from Taiwan cobra (*Naja naja atra*) venom. The known crystal structure of cardiotoxin V (chain A) was determined by [39] (ID No. 1KXI in the Protein Data Bank at http://www.rcsb.org) and is a member of the snake venom cytotoxin functional class of TFPs. Disulfide bonds are depicted in tan.

differences suggest that definitive structural analyses will be required in future studies to confirm the computational models.

In addition to the evolutionary conservation of eight cysteine residues, there are two important features of PMF that are shared with other members of the TFP superfamily: (a) a secretion signal peptide that is cleaved two residues before the first cysteine; (b) a signature sequence of C-C-X-X-[D]-X-C-N at the C-terminus (Fig. 1). Four residues (Leu6, Gly8, Lys25 and Glu30) present in 90% of PMF sequences correspond to the predicted tips of loop I and loop II, regions that are important for binding muscular nAChRs in α-neurotoxins (long and short chain) and neuronal nAChRs in κ-bungarotoxin (Fig. 1; consensus).

A comparison of PMF protein sequence with other TFPs highlights several additional features of PMF that may have functional implications. One key difference is predicted loop length. Compared with most TFPs, loop I of PMF is predicted to be shorter by 3–7 residues, loop II is estimated to be shorter by 4–8 residues, and, although loop III is the least conserved region in terms of both sequence composition and length, this loop appears to be longer than most TFPs by ≈7 residues (Fig. 1). Similarly to cardiotoxins and short neurotoxins, PMF also lacks the fifth disulfide bridge that forms in loop I of CD59 and nonconventional (weak) toxins, or in loop II in many of the long-chain neurotoxins. The N-linked glycosylation site (N-X-S/T) found in loop I of membrane-bound TFPs, such as CD59, is absent from PMF. In addition, PMF lacks the C-terminal tail of some snake toxins and the glycosylphosphatidylinositol anchor of the membrane-bound TFP members. Lastly, most TFPs are basic whereas PMF is very acidic (Fig. 4A; supplementary Table S1). Approximately 85% of the PMF sequences have a predicted pI of 3.5–4.0, with 10.5% having pIs above 4.0 and 4.5% having pIs less than 3.5 (Fig. 4B). In contrast, pIs of snake venom TFPs range from 7.5 to 9.0, and CD59 pIs range between 5.0 and 7.8.

Discussion

A new, hypervariable class of TFPs

When analyzed with structural modeling software, the proteins encoded by PMF predict structural features that are consistent with the three-finger conformation characteristic of proteins belonging to the TFP superfamily. Members of this group include snake venom toxins (three-finger toxin), as well as a whole host of nontoxin TFPs isolated from birds, fishes, amphibians and mammals. These proteins are members of the same superfamily, yet exhibit extraordinary functional diversity and target specificities (refer to [40] for original references). Despite these functional differences,
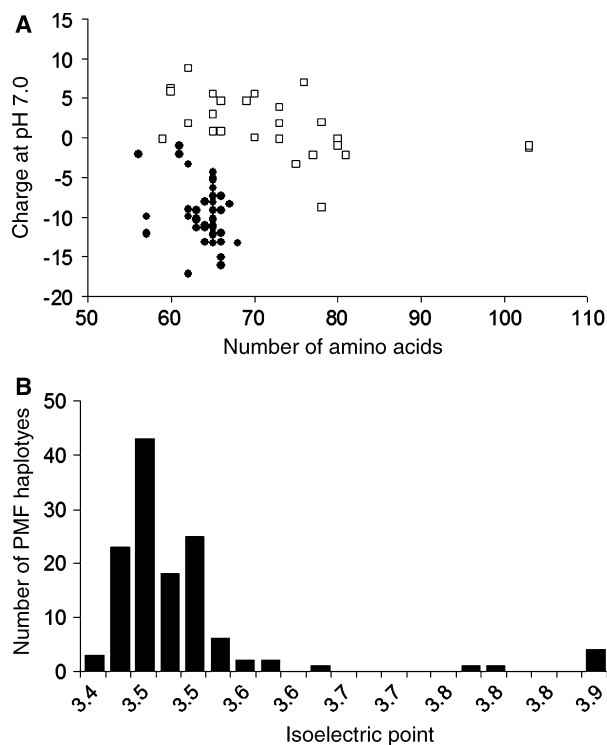
Fig. 4. (A) Net charge of TFPs at neutral pH. PMF sequences are depicted with black circles whereas white squares represent xenoxin, xlurp, slurp, rat spleen and urinary proteins, mouse seminal, ly6 and lynx proteins, human prostrate antigen, snake toxins, pig PIP protein and CD59. (B) Distribution of PMF amino-acid sequences based on derived pIs. For both (A) and (B), the known (from amino-acid sequencing of PMF) or predicted signal peptide (19 amino acids) was removed from PMF sequences before computation. See supplementary Table S1 for PMF data.

the individual members of the superfamily are generally found in single-copy number and exhibit low diversity [1,41,42]. The only significant exception to this picture is the family of snake neurotoxins and related toxin components, which are highly expressed in venom glands and exhibit broad sequence and functional diversity [6]. PMF represents a second class of TFPs that displays extraordinary sequence variation at both the nucleotide and amino-acid levels (average 18% and 35% sequence dissimilarity, respectively).

PMF and all members of the TFP superfamily share several important properties: (a) a characteristic hydrophobic secretion signal peptide which is cleaved two residues before the first cysteine; (b) eight similarly spaced cysteine residues; (c) a signature sequence C-C-X-X-[D]-X-C-N at the C-terminus. The eight cysteine residues form a pattern of disulfide bridges that results in a fold resembling three fingers extending

from a compact globular core (Fig. 3). The conserved asparagine at the end of the signature sequence plays an important role in the stabilization of TFPs, as its side chain penetrates into the core of the protein where it participates in hydrogen bonding [31]. Asp54 is maintained across 90% of the PMF sequences and is present in most other TFPs. The Asp negative side chain probably stabilizes the conformation of the protein by forming a weak chemical bond with the N-terminus or C-terminus of the molecule [40]. The considerable sequence variation of PMF makes it difficult to predict which other residues might be structurally and functionally important. Mutagenesis studies of related TFPs suggest that most chemical modifications of amino acids across these proteins result in a reduction but not a complete loss of function, suggesting that several sites participate in receptor binding [32,40]. However, four amino-acid residues, predicted to lie at the tips of loops I and II, are conserved across 90% of the PMF sequences. Because conserved residues at the tips of the loops are vital for receptor binding in many snake toxins (refer to [40] for original references), we propose that future efforts to elucidate the structure/function relationships of PMF should initially focus on these relatively well-conserved residues.

PMF sequences differ substantially from other TFPs

Distinct differences in amino-acid sequence, predicted structural features and biological function suggest that PMF comprises a distinct multigene subfamily within the TFP superfamily. The three-finger fold characteristic of members of the superfamily constitutes a stable structure that is capable of interacting with a broad range of targets. The functional multiplicity of this relatively simple protein structure is acquired via differences in overall length, orientation and flexibility of the loops, as well as differences in amino-acid side chains and their spatial distributions [1,42,43]. Not only is amino-acid sequence identity between PMF and snake venom toxins low (25–30%), the predicted loops I and (especially) II of PMF are significantly shorter than the loops of snake venom toxins (Fig. 1). Although loop III is the most variable portion of the PMF molecule in terms of length and amino-acid composition, it is predicted to be longer than three-finger toxins by seven residues (Fig. 1).

Comparisons of PMF with nontoxin TFPs indicates that loop I in PMF is substantially shorter, and that it lacks the extra disulfide bond that is present in loop I of most nontoxin TFPs (Fig. 1) [32]. In addition, all

nontoxin, membrane-bound TFPs contain a sequence encoding a glycosylphosphatidylinositol anchor near the C-terminus, as well as an N-linked glycosylation site. PMF is secreted and, similarly to other soluble TFPs, lacks both of these features. Overall, PMF differs significantly from all other members of the TFP superfamily in terms of the predicted overall net charge at neutral pH. PMF has few basic residues and an abundance of asparagine and glutamate residues, resulting in a high net negative charge at neutral pH (pI range of most PMFs 3.5–4.0). Whereas PMF is very negatively charged at physiological pH, other TFPs tend to be positively charged.

A pheromone function for the TFP family

PMF is one of two major components of a proteinaceous courtship pheromone produced by the mental gland of male *P. shermani* [29]. In preliminary studies of the whole extract obtained from male mental glands, four members of this 7-kDa family of protein isoforms were partially purified and subjected to N-terminal amino-acid sequencing, permitting initial cloning efforts (unpublished data) that formed the basis for this investigation. Our RT-PCR survey and *in situ* labeling studies indicate that, although PMF is only highly expressed in the male gland, it is also present in the skin surrounding the vent and from the dorsal tail-base regions, as well as in the liver, intestine and kidney of salamanders of both sexes. Expression outside of the male gland is unusual for salamander pheromone genes [21,44]. Although PMF expression is widespread, labeling of PMF mRNA using ISH revealed a dramatic difference in the level of PMF transcript between the mental gland and the skin tissue from different areas of the adult male *P. shermani*. Extremely intense PMF ISH labeling was observed throughout most of the mental gland, whereas, in stark contrast, no PMF labeling was observed in the skin tissue. Attempts to resolve PMF labeling by extending (doubling) the exposure time of the tissue to the radiolabeled probe also failed to resolve the PMF ISH labeling in the skin. PMF mRNA is apparently strongly expressed in the male mental gland but at very low levels in the male and female skin. Additional evidence of overexpression in the gland comes from the results of the cDNA library, in which 40% of the randomly sequenced clones encoded PMF. Thus, unlike other plethodontid pheromone genes, PMF is expressed in a variety of tissues in both sexes. Similarly to other plethodontid pheromone genes, however, it is hyperexpressed in the male's mental gland [44].

The mode of action of PMF is not known

At present, the molecular basis of PMF function remains obscure. PMF substantially decreases sexual receptivity of female salamanders when it is experimentally delivered as a single, purified component [28]. The ability of PMF to alter female behavior during courtship is a unique function for TFPs. The application of PMF to the female's nares produces a significant response by vomeronasal neurons [25]. When PMF is delivered in combination with the second major pheromone component, PRF, female sexual receptivity is enhanced [45]. PRF also elicits a VNO response [24], indicating that pheromone detection in these salamanders occurs through the accessory olfactory system, a neural pathway known to initiate reproductive responses in other vertebrates (see review [26]). The diversity of PMF variants coupled with the multiple modes of action of TFPs suggests that PMF may have multiple endogenous targets. Regardless of mode of action, pheromone activity is a new function for the TFP family.

Experimental procedures

Animal and tissue collection

Plethodon shermani were collected during the breeding season (August) from a single locality in Macon County, NC, USA (35°10′ 48′-N; 083°33′ 38′-W) and transported to Oregon State University. After a 2-week acclimation period in the laboratory, male/female pairs were placed in courtship arenas and left undisturbed for a period of 12 h. Pairs that successfully mated during these courtship trials were included in this study. Tissues were excised from anesthetized animals [44] and stored individually at −80 °C. Tissue samples from adult animals included: liver, kidney, heart, tail tip, intestine, mental (chin) glands from males, skin from the chins of females, skin from the dorsal tail-base (DT) region and from around the vent of the cloaca (VT) of both sexes. In addition, the undissected bodies of two juvenile *P. shermani* (0.5–0.6 cm snout-to-vent length) were homogenized and individually stored. All procedures were performed under the guidelines of the Public Health Service *Policy on Humane Care and Use of Laboratory Animals* [45a] and approved by the Oregon State University Animal Care and Use Committee.

DNA sequencing

Two different approaches were used to generate two sets of PMF sequences: (a) a cDNA library; (b) RT-PCR using specific primers. The cDNA library was constructed from the mental glands of 10 male *P. shermani*, and 300 clones were randomly sequenced [44]. A primer pair (P7NF, 5′-CACCTGGAATCCAGAATGA-3′; P7NR, 5′-AAGAG TGTGTGACTAGTTGCAGA-3′) was designed from the conserved untranslated regions of PMF sequences taken from the cDNA library. RT-PCR was then performed on individual tissues as follows: total RNA was extracted from the tissues and reverse-transcribed into first-strand cDNA as described by Palmer *et al.* [44]. A 50-μL PCR was prepared with 1 μL cDNA, 2.5 U *Taq* polymerase, 5 μL 10 × buffer, 0.2 mM each dNTP, 2.5 mM MgCl$_2$, and 100 pmol of each primer. Amplification was carried out using initial denaturation at 95 °C for 3 min, 40 cycles of denaturation at 95 °C for 1 min, primer annealing at 51 °C for 45 s, an extension at 72 °C for 1 min, and one final extension at 72 °C for 10 min. Amplified PCR products were purified from agarose gels, cloned, and sequenced in both directions as described by Watts *et al.* [46].

Sequence analyses

Database searches were performed using both the BLAST and FASTA algorithms of the GenBank database. PMF protein structure predictions were performed using Rapid Protein Threading by Operation Research Technique (RAPTOR, version 3.0 [38]) and the Insight II homology modeling program, MODELER (Accelrys Software, Inc., San Diego, CA, USA; http://www.accelrys.com/products/insight/). The BIOEDIT sequence alignment editor was used for sequence alignments and editing [47]. Nucleotide sequences were translated to amino-acid sequences and then aligned using the CLUSTAL W algorithm. Minor adjustments were made manually before back-translation.

Nucleotide-by-nucleotide and protein distance estimation methods in the MEGA2 computer package (version 2.1 [48]) were used to estimate average nucleotide sequence dissimilarity (Tamura-Nei method) and average amino-acid sequence dissimilarity (with Poisson correction). Standard errors were determined using 500 bootstrap replicates. Protein isoelectric properties were determined computationally using the EDITSEQ program from DNAStar Inc. (Madison WI, USA).

In situ hybridization

A 255-bp cRNA probe was synthesized from the full-length ORF of *P. shermani* (PsherPMF24; accession number DQ882274). A large-scale PMF plasmid preparation was performed by alkaline lysis [49,50]. The plasmid was linearized with either *Spe*I or *Not*I restriction enzymes and used as a template for *in vitro* transcription using T7 or T3 polymerases to produce sense and antisense probes, respectively. Probes were extracted with phenol/chloroform (pH 5.2) followed by ethanol precipitation in the presence of 0.4 M NaCl. The probes were then resuspended in 0.1% SDS and stored at −80 °C.

Three adult animals were anesthetized as described above, and mental gland and skin tissue (VT and DT) were

removed, embedded in Histoprep Frozen Tissue Embedding Medium (Fisher Scientific, Pittsburgh, PA, USA), and stored at −80 °C until sectioned. Tissue was sectioned at a 20 μm thickness at −20 °C on a cryostat. Two whole juvenile salamanders were sliced in frontal sections. All tissue was thaw-mounted on Superfrost Plus® positive-charged microscope slides (Shandon, Inc., Pittsburgh, PA, USA), and stored at −80 °C. ISH followed the methods of Zoeller *et al.* [51]. Tissue was fixed in 4% paraformaldehyde, rinsed in $1 \times NaCl/P_i$, and followed with acetylation in 0.45% NaCl containing 0.1 M triethanolamine hydrochloride (pH 8.0) and 0.25% acetic anhydride, then rinsed [$1 \times$ standard saline citrate (NaCl/Cit)]. The tissue was then dehydrated with ethanol, delipidated in chloroform, and partially rehydrated in ethanol. After being dried, the tissue was covered in hybridization solution (50% deionized formamide, 0.1% sodium pyrophosphate, 10% dextran sulfate, $2 \times NaCl/Cit$, 25 μg·mL^{-1} tRNA, $1 \times$ Denhardt's solution, and 200 mM dithiothreitol) containing the labeled probe and incubated for 20 h at 52 °C.

After incubation, the tissue was washed ($1 \times NaCl/Cit$), incubated in $2 \times NaCl/Cit/50\%$ deionized formamide (52 °C), and rinsed ($2 \times NaCl/Cit$). The tissue was then incubated in RNase wash buffer (0.5 M NaCl, 0.01 M Tris/HCl, 1 mM EDTA; pH 8.0) at 37 °C, then Rnase A (Sigma, St Louis, MO, USA; 100 μg·mL^{-1} in RNase wash buffer) at 37 °C, rinsed ($2 \times NaCl/Cit$), incubated ($2 \times NaCl/Cit/50\%$ deionized formamide; 52 °C), washed ($1 \times NaCl/Cit$), and ethanol (70%) dehydrated. Slides were dipped in Kodak NTB-2 emulsion film (Rochester, NY, USA) at 42 °C, dried, and exposed for 5 days at 4 °C. After exposure, tissue was developed and counterstained (0.1% methyl green), washed (tap water), and dehydrated in ethanol (50%) before being cover-slipped in Permount Histological Mounting Medium (Fisher Scientific).

Acknowledgements

References

1 Tsetlin V (1999) Snake venom alpha-neurotoxins and other 'three-finger' proteins. *Eur J Biochem* **264**, 281–286.

2 Kini RM (2002) Molecular moulds with multiple missions: functional sites in three-finger toxins. *Clin Exp Pharmacol Physiol* **29** (9), 815–822.

3 Nirthanan S, Gopalakrishnakone P, Gwee MCE, Khoo HE & Kini RM (2003) Non-conventional toxins from Elapid venoms. *Toxicon* **41**, 397–407.

4 Alape-Giron A, Persson B, Cederlund E, Flores-diaz M, Gutierrez JM, Thelestam M, Bergman T & Jornvall H (1999) Elapid venom toxins: multiple recruitments of ancient scaffolds. *Eur J Biochem* **259**, 225–234.

5 Fry BG, Wuster W, Kini RM, Brusic V, Khan A, Venkataraman D & Rooney AP (2003) Molecular evolution of elapid snake venom three finger toxins. *J Mol Evol* **57**, 110–129.

6 Fry BG & Wüster W (2004) Assembling an arsenal: origin and evolution of the snake venom proteome inferred from phylogenetic analysis of toxin sequences. *Mol Biol Evol* **21**, 870–883.

7 Fry BG, Vidal N, Norman JA, Vonk FJ, Scheib H, Ramjan SF, Kuruppu S, Fung K, Hedges SB, Richardson MK *et al.* (2006) Early evolution of the venom system in lizards and snakes. *Nature* **439**, 584–588.

8 Changeux JP, Kasai M & Lee CY (1970) Use of a snake venom toxin to characterize the cholinergic receptor protein. *Proc Natl Acad Sci USA* **67**, 1241–1247.

9 Rodriguez-Ithurralde D, Silveira R, Barbeito L & Dajas F (1983) Fasciculin, a powerful anticholinesterase polypeptide from *Dendroaspis angusticeps* venom. *Neurochem Int* **5**, 267–274.

10 Segalas I, Roumestand C, Zinn-Justin S, Gilquin B, Menez R, Menez A & Toma F (1995) Solution structure of a green mamba toxin that activates muscarinic acetylcholine receptors, as studied by nuclear magnetic resonance and molecular modeling. *Biochemistry* **34**, 1248–1260.

11 Su S-H, Su S-J, Lin S-R & Chang K-L (2003) Cardiotoxin-III selectivity enhances activation induced apoptosis of human CD8+ T lymphocytes. *Toxicol Appl Pharmacol* **193**, 97–105.

12 Fischer J, Bouadjar B, Heilig R, Huber M, Lefevre C, Jobard F, Macari F, Bakija-Konsuo A, Ait-Belkacem F, Weissenbach J *et al.* (2001) Mutations in the gene encoding SLURP-1 in Mal de Meleda. *Hum Mol Genet* **10**, 875–880.

13 Macleod RJ, Lembessis P, James S & Bennett HP (1998) Isolation of a member of the neurotoxin/cytotoxin peptide family from *Xenopus laevis* skin which activates dihydropyridine-sensitive Ca^{2+} channels in mammalian epithelial cells. *J Biol Chem* **273**, 20046–20051.

14 Coronel CE, Winnica DE, Novella ML & Lardy HA (1992) Purification, structure and characterization of caltrin proteins from seminal vesicle of the rat and mouse. *J Biol Chem* **267**, 20909–20915.

15 Morgan BP (1999) Regulation of the complement membrane attack pathway. *Crit Rev Immunol* **19**, 173–198.

16 Lee S-K, Su B, Maher SE & Bothwell ALM (1994) Ly-6A is required for T cell receptor expression and protein tyrosine kinase fyn activity. *EMBO J* **13**, 2167–2176.

17 Zammit DJ, Berzins SP, Gill JW, Randle-Barrett ES, Barnett L, Koentgen F, Lambert GW, Harvey RP, Boyd RL & Classon BJ (2002) Essential role for the lymphostromal plasma membrane Ly-6 superfamily molecule thymic shared antigen 1 in development of the embryonic adrenal gland. *Mol Cell Biol* **22**, 946–952.

18 Sidenius N & Blasi F (2003) The urokinase plasminogen activator system in cancer: recent advances and implication for prognosis and therapy. *Cancer Metastasis Rev* **33**, 205–222.

19 Miwa JM, Ibanez-Tallon I, Crabtree GW, Sanches R, Sali A, Role LW & Heintz N (1999) Lynx1, an endogenous toxin-like modulator of nicotinic acetylcholine receptors in the mammalian CNS. *Neuron* **23**, 105–114.

20 Rollmann SM, Houck LD & Feldhoff RC (1999) Proteinaceous pheromone affecting female receptivity in a terrestrial salamander. *Science* **285**, 1907–1909.

21 Palmer CA, Watts RA, Houck LD, Picard AL & Arnold SJ (2007) Evolutionary replacement of components in a salamander pheromone signaling complex: more evidence for phenotypic-molecular decoupling. *Evolution* **61**, 202–215.

22 Arnold SJ (1976) Sexual behavior, sexual interference, and sexual defense in the salamanders *Ambystoma maculatum*, *Ambystoma tigrinum* and *Plethodon jordani*. *Z Tierpsychol* **42**, 247–300.

23 Dawley EM & Bass AH (1989) Chemical access to the vomeronasal organs of a salamander. *J Morphol* **200**, 163–174.

24 Wirsig-Wiechmann CR, Houck LD, Feldhoff PW & Feldhoff RC (2002) Pheromonal activation of vomeronasal neurons in plethodontid salamanders. *Brain Res* **952**, 335–344.

25 Wirsig-Wiechmann CR, Houck LD, Wood JM, Feldhoff PW & Feldhoff RC (2006) Male pheromone protein components activate female vomeronasal neurons in the salamander *Plethodon shermani*. *BMC Neurosci* **7**, 26.

26 Halpern M & Martinez-Marcos A (2003) Structure and function of the vomeronasal system: an update. *Prog Neurobiol* **70**, 245–318.

27 Laberge F & Roth G (2005) Connectivity and cytoarchitecture of the ventral telencephalon in the salamander *Plethodon shermani*. *J Comp Neurol* **482**, 176–200.

28 Houck LD, Palmer CA, Watts RA, Arnold SJ, Feldhoff PW & Feldhoff RC (2007) A new vertebrate courtship pheromone that affects female receptivity in a terrestrial salamander. *Anim Behav* **73**, 315–320.

29 Feldhoff RC, Rollmann SM & Houck LD (1999) Chemical analyses of courtship pheromones in a plethodontid salamander. In *Advances in Chemical Communication in Vertebrates* (Johnston RE, Muller-Schwarze D & Sorensen P, eds), pp. 117–125. Plenum Press, New York, NY.

30 Rollmann SM, Houck LD & Feldhoff RC (2000) Population variation in salamander courtship pheromones. *J Chem Ecol* **26**, 2713–2724.

31 Betzel C, Lange G, Pal GP, Wilson KS, Maelicke A & Saenger W (1991) The refined crystal structure of alpha-cobratoxin from *Naja naja siamensis* at 24-Å resolution. *J Biol Chem* **266**, 21530–21536.

32 Petranka J, Zhao J, Norris J, Tweedy NB, Ware RE, Sims PJ & Rosse WF (1996) Structure-function relationships of the complement regulatory protein, CD59. *Blood Cells Mol Dis* **22**, 281–296.

33 Pillet L, Trémeau O, Ducancel F, Drevet P, Zinn-Justin S, Pinkasfeld S, Boulain J-C & Ménez A (1993) Genetic engineering of snake toxins: role of invariant residues in the structural and functional properties of a curaremimetic toxin, as probed by site-directed mutagenesis. *J Biol Chem* **268**, 909–916.

34 Rees B & Bilwes A (1993) Three-dimensional structures of neurotoxins and cardiotoxins. *Chem Res Toxicol* **6**, 385–406.

35 Zhao X-J, Zhao J, Zhou Q & Sims PJ (1998) Identity of the residues responsible for the species-restricted complement inhibitory function of human CD59. *J Biol Chem* **273**, 10665–10671.

36 Zhang H-FYuJ, Chen S, Morgan BP, Abagyan R & Tomlinson S (1999) Identification of the individual residues that determine human CD59 species selective activity. *J Biol Chem* **274**, 10969–10974.

37 Michalet S, Teixeira F, Gilquin B, Mourier G, Servent D, Drevet P, Binder P, Tzartos S, Ménez A & Kessler P (2000) Relative spatial position of a snake neurotoxin and the reduced disulphide bond α (Cys^{192}-Cys^{193}) at the $\alpha\gamma$ interface of the nicotinic acetylcholine receptor. *J Biol Chem* **275**), 25608–25615.

38 Xu J, Li M, Kim D & Xu Y (2003) RAPTOR: optimal protein threading by linear programming. *J Bioinform Comput Biol* **1**, 95–117.

39 Sun YJ, Wu WG, Chiang CM, Hsin AY & Hsiao CD (1997) Crystal structure of cardiotoxin V from Taiwan cobra venom: pH-dependent conformational change and a novel membrane-binding motif identified in the three-finger loops of P-type cardiotoxin. *Biochemistry* **36**, 2403–2413.

40 Nirthanan S & Gwee MC (2004) Three-finger alpha-neurotoxins and the nicotinic acetylcholine receptor, forty years on. *J Pharmacol Sci* **94**, 1–17.

41 Adermann K, Wattler F, Wattler S, Heine G, Meyer M, Frossmann W-G & Nehls M (1999) Structural and

phylogenetic characterization of human SLURP-1, the first secreted mammalian member of the Ly-6/uPAR protein superfamily. *Protein Sci* **8**, 810–819.

42 Ricciardi A, le Du MH, Khayati M, Dajas F, Boulain JC, Menez A & Ducancel F (2000) Do structural deviations between toxins adopting the same fold reflect functional differences? *J Biol Chem* **275**, 18302–18310.

43 le Du MH, Marchot P, Bougis PE & Fontecilla-Camps JC (1992) 19-Å resolution structure of fasciculin 1, an anti-acetylcholinesterase toxin from green mamba snake venom. *J Biol Chem* **267**, 22122–22130.

44 Palmer CA, Watts RA, Gregg RG, McCall MA, Houck LD, Highton R & Arnold SJ (2005) Lineage-specific differences in evolutionary mode in a salamander courtship pheromone. *Mol Biol Evol* **22**, 2243–2256.

45 Houck LD, Bell AM, Reagan-Wallin NL & Feldhoff RC (1998) Effects of experimental delivery of male courtship pheromones on timing of courtship in a terrestrial salamander, *Plethodon jordani* (Caudata: Plethodontidae). *Copeia* **1998**, 214–219.

45a Public Health Service (2002) *Policy on humane care and use of laboratory animals*. Office of Laboratory Animal Welfare, National Institutes of Health, Bethesda, MD.

46 Watts RA, Palmer CA, Feldhoff RC, Feldhoff PW, Houck LD, Jones AG, Pfrender ME, Rollmann SM & Arnold SJ (2004) Stabilizing selection on behavior and morphology masks positive selection on the signal in a salamander pheromone signaling complex. *Mol Biol Evol* **21**, 1032–1041.

47 Hall TA (1999) Bioedit: a user friendly biological sequence alignment, ed. and analysis program for Windows 95/97/NT. *Nucleic Acids Symposium Series* **41**, 95–98.

48 Kumar S, Tamura K, Jakobsen IB & Nei M (2001) MEGA2: molecular evolutionary genetics analysis software. *Bioinformatics* **17**, 1244–1245.

49 Birnboim HC & Doly J (1979) A rapid alkaline extraction procedure for screening recombinant plasmid DNA. *Nucleic Acids Res* **7**, 1513–1523.

50 Maniatis T, Fritsch EF & Sambrook J (1982) *Molecular Cloning: A Laboratory Manual*. Cold Spring Harbor Laboratory Press, Cold Spring Harbor, NY.

51 Zoeller RT, Fletcher DL, Butnariu O, Lowry CA & Moore FL (1997) *N*-Ethylmaleimide (NEM) can significantly improve *in situ* hybridization results using ^{35}S-labeled oligodeoxynucleotide or complementary RNA probes. *J Histochem Cytochem* **45**, 1035–1041.

Supplementary material

The following supplementary material is available online:

Table S1. Detailed characteristics of PMF sequences from *P. shermani*.

Fig. S1. Sequence alignment for *P. shermani* PMF proteins.

This material is available as part of the online article from http://www.blackwell-synergy.com

Please note: Blackwell Publishing is not responsible for the content or functionality of any supplementary materials supplied by the authors. Any queries (other than missing material) should be directed to the corresponding author for the article.